Journal of Alloys and Compounds 509 (2011) 6400–6407

Contents lists available at ScienceDirect

Journal of Alloys and Compounds

journal homepage: www.elsevier.com/locate/jallcom

# Synthesis and high temperature XRD studies of tantalum nitride thin films prepared by reactive pulsed dc magnetron sputtering

T. Elangovan [a], S. Murugeshan [b], D. Mangalaraj [c,*], P. Kuppusami [b], Shabhana Khan [b], C. Sudha [b], V. Ganesan [d], R. Divakar [b], E. Mohandas [b]

[a] Thin Film and Nanomaterials Laboratory, Department of Physics, Bharathiar University, Coimbatore-641 046, India
[b] Physical Metallurgy Division, Indira Gandhi Centre for Atomic Research, Kalpakkam-603 102, India
[c] Department of Nanoscience and Technology, Bharathiar University, Coimbatore-641 046, India
[d] UGC-DAE CSR, Indore-452 017, India

ARTICLE INFO

*Article history:*
Received 15 November 2010
Received in revised form 9 March 2011
Accepted 11 March 2011
Available online 21 March 2011

*Keywords:*
Thin films
Thermal expansion
X-ray diffraction
Transmission Electron Microscopy
High-temperature alloys

ABSTRACT

In the present work, the growth characteristics of tantalum nitride (TaN) thin films prepared on (1 0 0) Si substrates by reactive pulsed DC magnetron sputtering are investigated. XRD analyses indicated the presence of α-Ta and β-Ta in the films deposited in pure argon atmosphere, while β-TaN and fcc-TaN phases appeared for 2 sccm of nitrogen, and cubic TaN for 5–25 sccm of nitrogen in the sputtering gas mixture of argon and nitrogen at a substrate temperature of 773 K. The TaN films obtained with increasing substrate temperature and pulse width showed a change in the texture from [1 1 1] to [2 0 0] orientation. Atomic force microscopy (AFM) results indicated that the average surface roughness was low for films deposited in pure argon than for the films deposited in a mixed $Ar + N_2$ atmosphere. Nanocrystalline phase of the deposited material was identified from the high-resolution transmission electron microscopy (HRTEM) images. X-ray photoelectron spectroscopy (XPS) core level spectra confirmed the formation of TaN phase. The high temperature X-ray diffraction analysis of the optimized TaN thin film was performed in the temperature range 298–1473 K. The lattice parameter of the TaN films was found to increase from 4.383 to 4.393 Å on increasing the temperature from 298 to 823 K and it reduced to 4.345 Å at 1473 K. The thermal expansion coefficient value was found to be negative for the TaN films.



## 1. Introduction

Transition-metal nitrides are of great interest for structural applications owing to their physical and chemical properties [1,2]. Tantalum nitride has received particular interest in recent years because of its inherent properties, such as good thermal stability and low electrical resistivity [3]. Consequently tantalum nitride thin films have been recently developed for microelectronic applications as efficient diffusion barriers in Cu-based metallization. TaN exhibits different stable phases such as bcc-TaN, hcp-$Ta_2N$, fcc-TaN, hexagonal-TaN, hexagonal-$Ta_5N_6$, tetragonal-$Ta_4N_5$ and orthorhombic-$Ta_3N_5$ [4], with differing physical, chemical and mechanical properties depending on the growth conditions. In general, these films are grown by physical and chemical vapour deposition techniques [5–8]. Because tantalum nitride has a defective structure, variations in stoichiometry are common in these films. Consequently, the properties of the films, e.g. microstructure and electrical resistivity, strongly depend on the deposition conditions. In the case of the DC reactive sputter deposition of coatings, the main problem is the formation of an insulating film on the target surface when an elemental metal target is sputtered in a mixture of argon and reactive gas. This so-called target poisoning could create micro particles over the target surface area. These micro particles may reach the substrate and become imbedded in the growing film. This problem had been technologically overcome by using pulsed DC power supplies [9]. These power supplies are known to provide higher ionization rates without target poisoning and can improve the film quality by decreasing the amount of macro particles caused by micro arcs. The study on the dependence of the process parameters on the growth of TaN by pulsed magnetron sputtering is very scarce [10].

Thermal expansion is one of the fundamental physical properties for materials science and engineering. Determination of linear thermal expansion coefficient and thermal effect of TaN has recently attracted the attention of many researchers. Tantalum nitride is a strong candidate for advanced structural applications at high temperatures, because it has a high melting point, good creep resistance, superior high temperature strength, low thermal expansion, outstanding thermal shock resistance and displays exceptional chemical stability under harsh chemical environments.

* Corresponding author. Tel.: +91 0422 2425458; fax: +91 422 2422387.
*E-mail address:* dmraj800@yahoo.com (D. Mangalaraj).

0925-8388/$ – see front matter © 2011 Elsevier B.V. All rights reserved.
doi:10.1016/j.jallcom.2011.03.067

In an earlier work, Terao reported the formation of several phases of tantalum nitride on nitriding evaporated Ta films in an atmosphere of ammonia and nitrogen. He also studied the effect of variation of temperature in the range of 600–1100 °C (873–1375 K) to achieve $TaN_{0.5}$, $Ta_2N$, d-TaN, e-TaN, $Ta_5N_6$, $Ta_4N_5$, and $Ta_3N_5$ phases [11]. Shin et al. obtained a series of lower nitrides, like $TaN_{0.1}$, $Ta_4N$ and $Ta_2N$ by reactive magnetron sputtering Ta as a function of the $N_2$ pressure over MgO (0 0 1) and oxidized Si (0 0 1) at low pressures. At higher $N_2$ pressures and temperatures of 566–634 °C (823–923 K) he observed a mixture of rocksalt TaN*x* and body-centered-tetragonal TaN*x* structures [12]. However in the present work, a systematic study of the influence of nitrogen flow rate and substrate temperature on the growth of TaN films prepared by pulsed DC magnetron sputtering has been carried out to understand their structure and microstructure over a wide range of substrate temperatures and nitrogen flow rates. We have studied the microstructure and the thermal stability of the TaN film in the temperature range of 298–1373 K.

## 2. Experimental procedures

Tantalum nitride films were deposited by reactive DC magnetron sputtering from a 76 mm diameter Ta target of 99.9% purity. The magnetron was driven by a 5-kW pulsed dc power supply (ENI RPG 100A) with a pulsing frequency of 100 kHz and duty cycle of 26%. The deposition chamber was pumped down to a base pressure of $2 \times 10^{-6}$ mbar by using Alcatel make rotary and turbo molecular pumps. MKS mass flow controllers were used to regulate the flow rate of argon (99.999%) and nitrogen (99.99%) gases. All the depositions were carried out at a working pressure of $\sim 8 \times 10^{-3}$ mbar for a constant duration of 40 min. A halogen lamp (800 W, 6.3A) heater, a chromel–alumel thermocouple and a digital temperature programmer/controller were used to maintain the substrates at the required temperature. One side polished P-doped Si (1 0 0) wafers were used as the substrates. All substrates were ultrasonically pre-cleaned in acetone. Prior to deposition of the TaN films, the target was sputter-cleaned for about 10 min. The deposited TaN films were characterized by X-ray diffraction (XRD) using (INEL XRG – 3000 fitted with CPS590 curved position sensitive detector) a glancing angle of incidence ($\omega$) of 5°. The lattice parameters of both TaN were determined using unit cell program. The crystallite size of the films was calculated from the FWHM values using the Scherrer equation, $D = K\lambda/\beta \cos\theta$; where $D$ is the average crystallite size, $K$ is the constant (=0.9 assuming that the particles are spherical shape), $\lambda$ is the wavelength of Cu Kα X-ray radiation (1.54056 Å), $\theta$ is the angle of diffraction, $\beta = \sqrt{B^2 - b^2}$ is the full width at half maximum of peak (FWHM), $B$ is FWHM obtained from the films, and $b$ is FWHM due to instrumental broadening calculated from Si standard. Texture coefficients (TC) of (1 1 1) and (2 0 0) reflections were determined from the intensities of TaN peaks. In general (Eq. (1)), the TC for any reflection can be determined using the relation:

$$TC = \frac{I_m(h\ k\ l)I_0(h\,k\,l)}{(1/n)\sum\{I_m(h\,k\,l)/I_0(h\,k\,l)\}} \quad (1)$$

where $n$ is the number of peaks, $I_m$ is the measured peak intensities reflections of TaN films, and $I_0$ is the respective peak intensities corresponding to the bulk TaN data from JCPDS File No: 49-1283. Surface morphology of the films was examined using an atomic force microscope (Digital Instruments Inc, Nanoscope E, US). XPS experiments were carried out using Al Kα X-ray source (1486.6 eV) and the data were collected by a 150 mm (mean radius) hemispherical analyzer at 20 eV pass energy. The samples for transmission electron microscopy (TEM) were prepared by back-thinning the substrate to electron transparency by mechanical polishing and ion-milling. TEM studies were carried out on a Philips CM 200 and JEOL 2000 EX-II TEM operated at 200 kV. High temperature X-ray diffraction studies were performed in INEL make XRG 3000 model diffractometer equipped with curved position sensitive detector using Cu K( radiation. X-ray monochromatic radiation of Cu $K_{\alpha 1}$ (wavelength = 1.54056 Å) was used in these studies. Buhler HDK 2.4 high temperature camera with Ta as a heating holder was used for the high temperature measurements in the two theta range of 20–90°. The chamber was maintained at a pressure of $2.8 \times 10^{-6}$ mbar throughout the experiment. The thermal properties were studied in the temperature range of 298–1373 K at a heating rate of 10 K per minute.

## 3. Results and discussion

### 3.1. Influence of nitrogen flow rate

Fig. 1 shows the effect of nitrogen flow rate on the X-ray diffraction patterns of the tantalum nitride films deposited on Si (1 0 0).

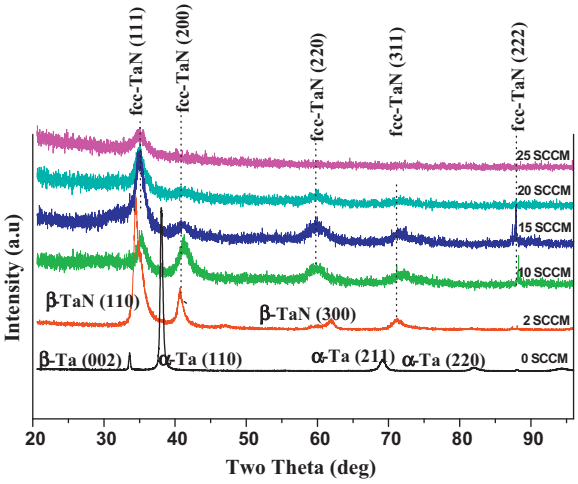


**Fig. 1.** X-ray diffraction patterns of TaN films deposited at 773 K on Si (1 0 0) at different substrates at different nitrogen flow rates.

The α-Ta (JCPDS Card No: 04-788) is identified from the (1 1 0) (2 1 1) and (2 2 0) reflections. Also the β-Ta (JCPDS Card No: 25-1280) is identified from the (1 1 0) reflection. At 2 sccm of nitrogen flow rate, a mixed β-TaN (JCPDS File No: 39-1485) and fcc-TaN (JCPDS File No: 49-1283) phases are identified. The hexagonal phase is found to be dominant compared to cubic phase at this flow rate. When the nitrogen flow rate is raised to 10 sccm, fcc-TaN becomes the major phase. It is noticed that the intensity of these reflections decrease, while a greater tendency of peak broadening is seen with the increase of nitrogen flow rates. At a flow rate of 25 sccm, only the (1 1 1) peak with decreased intensity is observed. Similar results were reported in transition metal nitrides synthesized at higher nitrogen flow rates [13,14]. The lattice parameter of TaN films values was calculated using the unit cell program. The lattice cell parameter decreases from 4.427 to 4.408 Å when the $N_2$ flow rate increases from 2 to 10 sccm (Fig. 2). These values are higher than that of the bulk [4.339 Å], indicating the presence of tensile stress in these films. The observed decrease of cell parameter with the increase of $N_2$ flow rate may be attributed to Ta vacancies generated during sputtering under $N_2$ conditions. The position of the (1 1 1) peak shifts to a lower diffraction angle for nitrogen flow rates >10 sccm. At above 10-sccm nitrogen flow rate, tantalum nitride films are over stoichiometric corresponding to higher lattice parameter [15]. It is seen in Fig. 3, that the crystallite size decreases while FWHM increases with increasing nitrogen flow rate for TaN

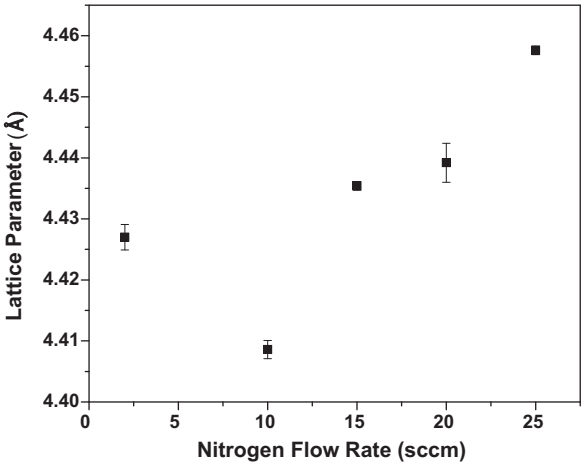


**Fig. 2.** Lattice parameter of TaN films deposited at 773 K at different $N_2$ flow rates.

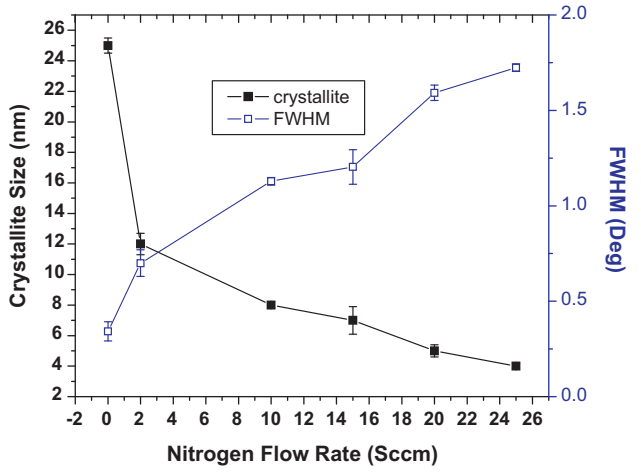


**Fig. 3.** FWHM and crystallite size of TaN films deposited at 773 K at different $N_2$ flow rates.

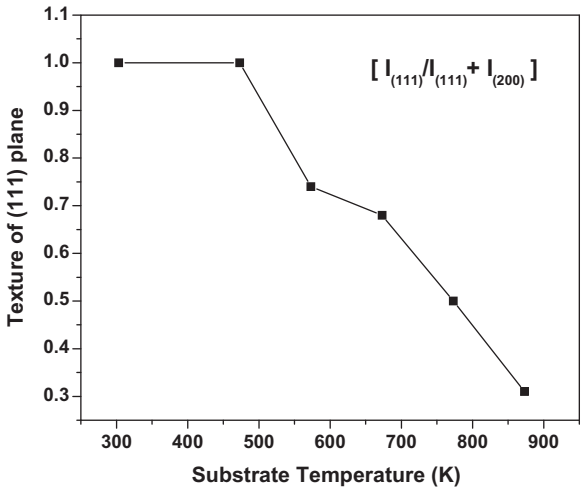


**Fig. 5.** Texture coefficient of the TaN films grown at 10 sccm on (1 0 0) Si substrates as a function of substrate temperature.

films. The deposited films have polycrystalline structure, and the crystallite size is inversely proportional to the full width at half maximum (FWHM) of diffraction peak. The crystallite size of the Ta formed in pure argon atmosphere is 25 nm. With the 2 sccm nitrogen flow rate, the crystallite size of TaN is determined as 15 nm. As the nitrogen flow rate increases to 10 sccm and above the crystallite size starts to and it reaches a value of 4 nm at 25 sccm of nitrogen. TaN phase may be inhibited because of the lattice strain induced by the excess nitrogen atoms. As a result, the grain size is significantly reduced with increasing $N_2$ flow rate.

### 3.2. Influence of substrate temperature

Fig. 4 shows the XRD pattern of TaN thin films prepared at different substrate temperatures at a constant nitrogen flow rate of 10 sccm. The film formed at temperatures ≥473 K has a preferred (1 1 1) orientation. Between the temperatures of 473 and 873 K, the films are polycrystalline in nature. At these temperatures, peaks corresponding to the (1 1 1), (2 0 0), (2 2 0) and (3 1 1) planes of cubic tantalum nitride are observed at $2\theta$ values of 35.75, 41.75, 60.36 and, 72.36° respectively. When the substrate temperature is increased to 873 K, the adatom surface mobility of the deposited atoms is further increased. It is expected that higher temperatures promote crystallite size and a change in preferred orientation [16]. For the films deposited with a substrate temperature of 873 K, the intensity of the (2 0 0) peak is higher than that of the (1 1 1) peak. The substrate temperature has a profound influence in the change of orientation from ⟨1 1 1⟩ to ⟨1 0 0⟩. Unlike CrN films, the increase in the crystallite size is not significant in the case of TaN films and is found to be in the range 5–7.6 nm [17]. The calculated value of $I_{111}/I_{111}+I_{220}$, which is a qualitative measure of (1 1 1) texture is depicted as a function of substrate temperature in Fig. 5. From this, we can know that the (1 1 1) texture was maintained up to 673 K and it decreased with the increasing substrate temperatures, which was similar to the results by Jung [18] and Hong et al. [19]. Knuyt et al. [20] proposed a model to explain the texture evolution in PVD thin films, which supposed that the only driving physical process for the texture evolution is the tendency of the surface to evolve towards a situation of lower surface energy. Generally during the initial stages of film growth, the nuclei have mixed orientation. After forming a continuous film the grains of (1 1 1) plane, which have lower surface energy, occupy more area of film surface at lower substrate temperature. For that reason the development of (1 1 1)-oriented grains would be promoted. However, when sufficient thermal energy is available, then, (2 0 0) texture becomes stronger and a similar tendency is also reported for CrN thin films [21].

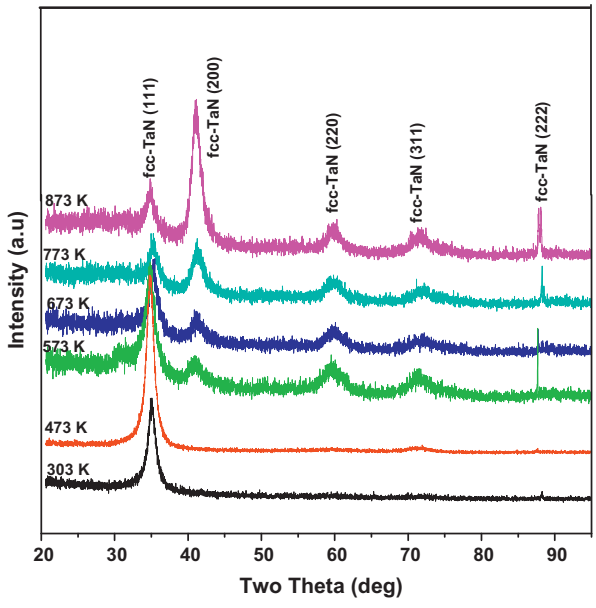


**Fig. 4.** XRD patterns of TaN films deposited on (1 0 0) Si at 10 sccm of nitrogen flow rate and at different substrate temperatures.

### 3.3. Surface morphology

The surface morphology of the TaN films studied by atomic force microscope (AFM) is shown in Fig. 6. It is found that the surface of the sample contains both cuboidal and elliptical shaped crystallites with the root mean square (RMS) roughness of 1.9 nm for the films deposited in pure argon atmosphere (Fig. 6(a)) [22]. When nitrogen was introduced into the chamber, the round shape grains were getting coarsening and the surface roughness was lightly increased (Fig. 6(b)). It is found that the RMS roughness increased to 7.576 nm for the TaN film ($N_2$ flow rate: 10 sccm). At this condition, the film morphology shows very fine shaped grains on the film surface (Fig. 6(c)). In addition, Lee et al. [23] revealed that the time average ion flux and energy fluxes increased as the pulse dc magnetron sputtering was used. With an increasing number of preferential nucleation sites, the grain size of thin film will be decreased which

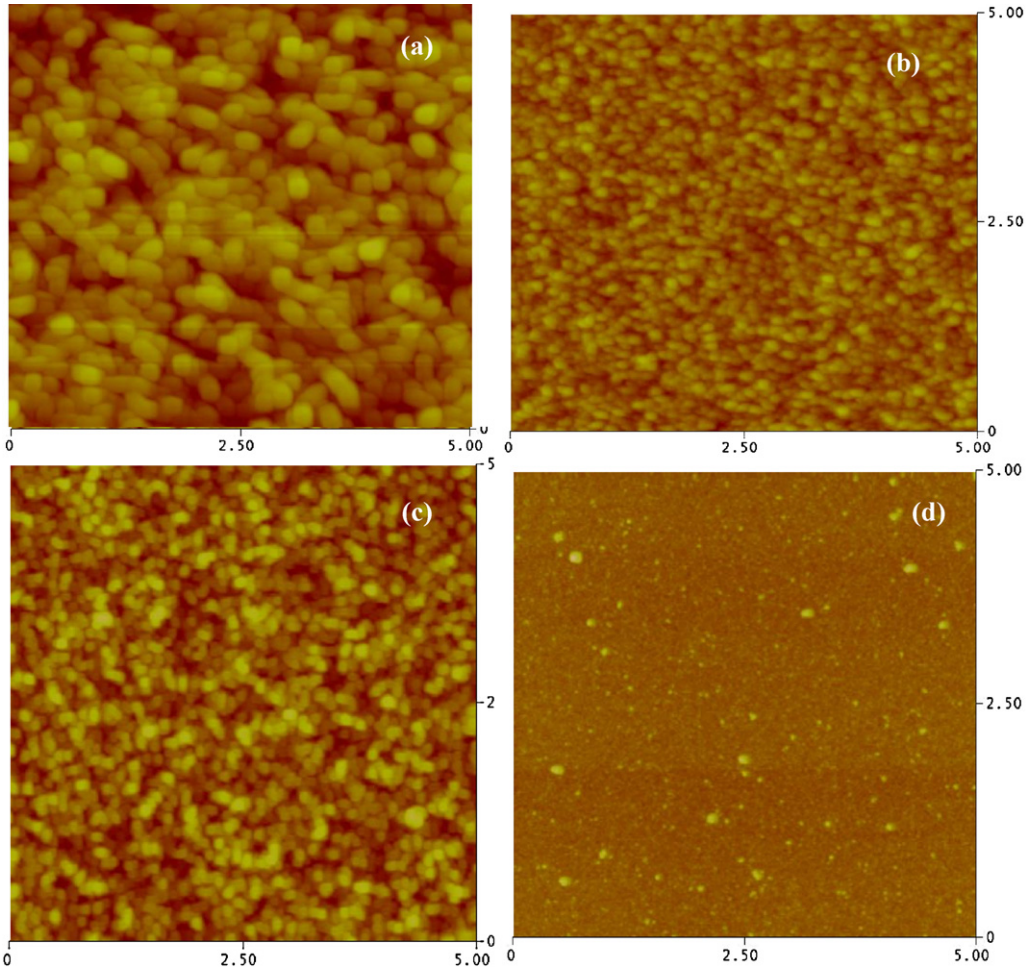


**Fig. 6.** AFM images of TaN films deposited at 773 K as a function of nitrogen flow rate (a) 0 (b) 2 (c) 10 and (d) 25 sccm.

will result in a smoothened film surface. At flow rate of 25 sccm, the film surface has lesser number of grains because of the film amorphous nature and this result is in accordance with the XRD pattern. Substrate temperature is considered as an important factor in deciding the shape and size of the crystallites of thin films [24]. At the low temperature of 303 K (Fig. 7(a)), the surface morphology of the film could not be observed clearly even at high magnifications due to increased nucleation compared to the rate of growth. With the increasing substrate temperature, the motion of adatoms will be improved and the crystallites grow bigger, accordingly the surface turns to be rougher. As the substrate temperature is raised from 303 to 573 K, the average grain size increases from 8.3 to 11.5 nm and the surface roughness increases from 4.2 to 6.6 nm. Well grown and mostly elliptical shaped crystallites are seen at 673 K, while the crystallites tend to faceting at 873 K.

### 3.4. XPS analysis of optimized TaN thin film

We have recently reported the chemical composition of TaN films with varying amounts of Cu using electron probe microanalysis [25]. The analysis indicated that the films prepared at the optimized conditions of deposition (773 K, 10 sccm of nitrogen) had Ta and N in the ratio 1:1. The chemical states of the elements were measured using XPS after 3 min of sputtering to avoid surface contamination on the film surface. The observed peaks were associated with Ta 4d and Ta 4f with binding energy in descending order. Weak intensities from O 1s, N 1s, and C 1s were also detected in the spectra. Furthermore, the chemical binding states of Ta were examined by narrow range scanning of XPS and the spectra are illustrated in Fig. 8. Both the spectra can be fitted by two sets of doublets. The spectra in Fig. 8(a) show the binding energy values of the low energy side doublets of Ta (Ta $4f_{7/2}$ = 23.875 eV and Ta $4f_{5/2}$ = 25.55 eV). These values are in good agreement with the values of TaN powders [26]. Zhang et al. [27] have reported a value of about 23.5 eV for the Ta $4f_{7/2}$ of cubic TaN film formed by ion beam assisted deposition. Lamour et al. reported similar XPS results for Ta position [28]. Fig. 8(b) shows the location of N 1s peak at 397.7 eV, implying the formation of N–Ta bonds.

### 3.5. TEM of optimized TaN thin film

Fig. 9 shows the plane-view bright field TEM and the corresponding diffraction patterns of the TaN films prepared at 10 sccm of $N_2$ flow rate and substrate temperature of 773 K. Single phase of NaCl-type structure with no other crystalline phase was found. Diffraction rings with (1 1 1), (2 0 0), (2 2 0), and (3 1 1) reflections of face-centered-cubic (fcc) TaN structure (inset of Fig. 9) are in agreement with the XRD results shown in Fig. 1. The dark field plane-view image depicted the round shaped morphology of the grains and the estimated grain size is ranging from 10 to 15 nm. The lattice planes can be uniquely identified as belonging to cubic TaN. The present result on the sputtered cubic phase of TaN films at 10 sccm of nitrogen flow rate is in good agreement with previous results reported by Tsukimoto et al. [14].

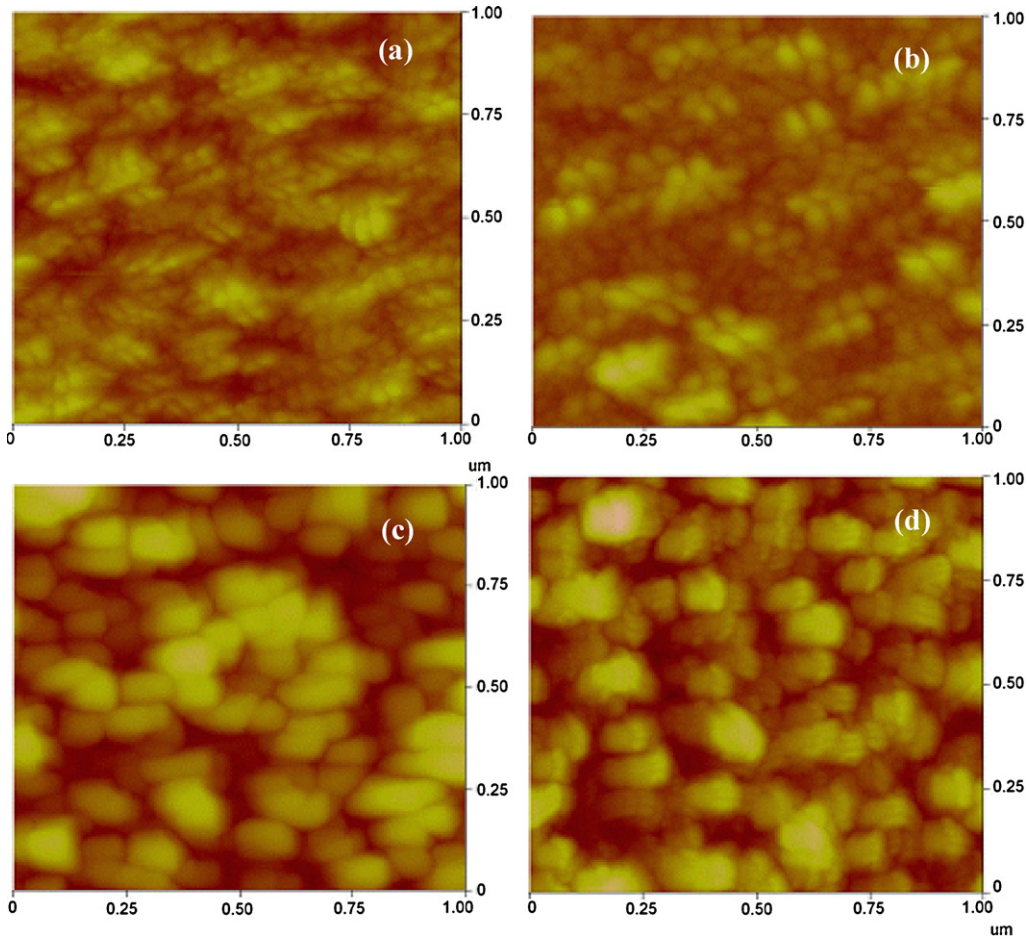


**Fig. 7.** AFM images of TaN films deposited at constant 10 sccm $N_2$ flow rate as a function subs temp (a) 303 (b) 473 (c) 673 and (d) 873 K.

### 3.6. High temperature studies of TaN film

Fig. 10 shows the high temperature X-ray diffraction (HTXRD) profiles of the TaN film prepared with 10 sccm of nitrogen flow rate at 773 K. The deposited film was recorded in the temperature range 298–1273 K after equilibrating the sample at each temperature for 10 min. The peaks corresponding to the (1 1 1), (2 0 0), (2 2 0) and (3 1 1) planes of cubic tantalum nitride could be observed throughout this temperature range, which indicate the good thermal stability of the fcc-TaN films prepared in the above condition. The phases were confirmed from the JCPDS #49-1283 for cubic tantalum nitride. At temperature of ≤723 K, the peaks appeared at 2$\theta$ angles of 35.41, 41.24, 59.93 and 71.85° corresponding to cubic tantalum nitride phase alone. It can be clearly seen that the cubic TaN retained its single phase for temperature up to 1273 K though a systematic but marginal shift of 2$\theta$ values towards a lower angle

**Table 1**
Fitted and corrected lattice parameter and coefficient of lattice thermal expansion in the temperature range of 298–1273 K.

| Temp | Temperature (K) | Lattice parameter (Å) | Fitted lattice parameter (Å) | Mean thermal expansion coefficients ($\times 10^{-5}$ K$^{-1}$) |
|---|---|---|---|---|
| 25 | 298 | 4.38387 | 4.3820 | |
| 50 | 323 | 4.38638 | 4.38452 | 2.45071 |
| 100 | 373 | 4.38806 | 4.38886 | 2.12886 |
| 150 | 423 | 4.39082 | 4.39238 | 1.91654 |
| 200 | 473 | 4.39107 | 4.39509 | 1.7201 |
| 250 | 523 | 4.3954 | 4.39701 | 1.53091 |
| 300 | 573 | 4.39672 | 4.39813 | 1.34414 |
| 350 | 623 | 4.39805 | 4.39847 | 1.16009 |
| 400 | 673 | 4.39973 | 4.39803 | 9.77666 |
| 450 | 723 | 4.40118 | 4.39681 | 7.96285 |
| 500 | 773 | 4.39877 | 4.39483 | 6.16584 |
| 550 | 823 | 4.39395 | 4.3921 | 4.38518 |
| 600 | 873 | 4.38854 | 4.38861 | 2.61259 |
| 650 | 923 | 4.38363 | 4.38438 | 8.53474 |
| 700 | 973 | 4.37693 | 4.37941 | −8.95182 |
| 750 | 1023 | 4.37098 | 4.37371 | −2.63239 |
| 800 | 1073 | 4.3648 | 4.36728 | −4.36037 |
| 850 | 1123 | 4.35911 | 4.36014 | −6.07526 |
| 900 | 1173 | 4.35473 | 4.35229 | −7.77931E−6 |
| 950 | 1223 | 4.34507 | 4.34373 | −9.47429E−6 |

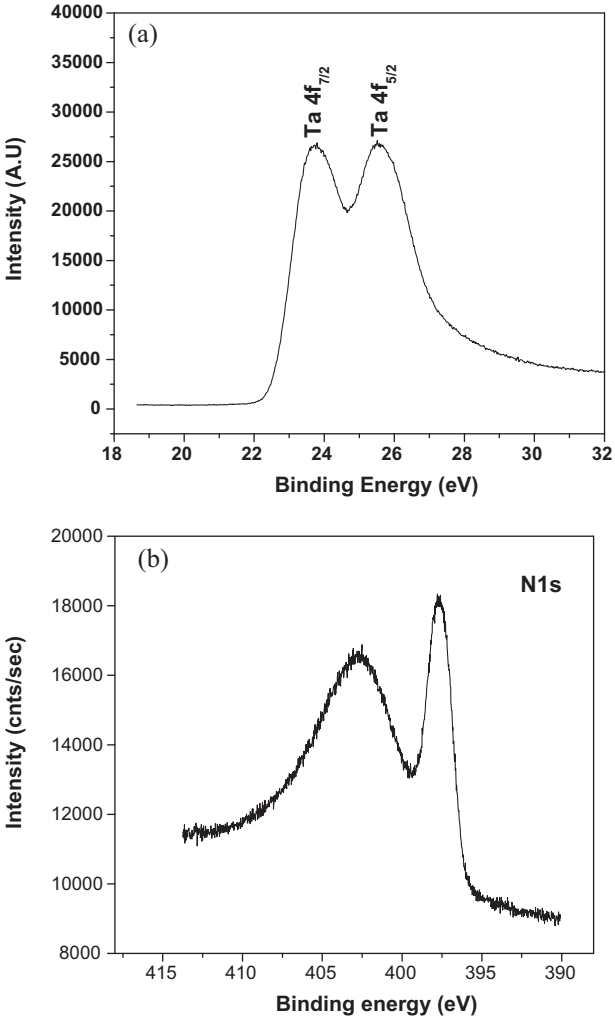


**Fig. 8.** XPS spectra of TaN films prepared at 773 K and 10 sccm of $N_2$ flow rate. (a) Ta $4f_{7/2}$ and (b) N 1s.

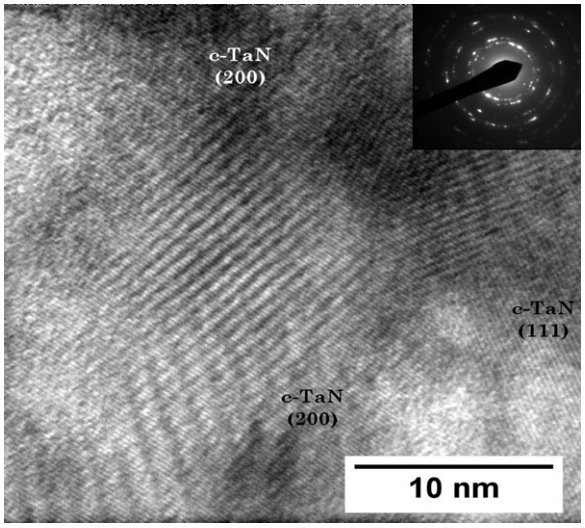


**Fig. 9.** TEM image of TaN films prepared at 773 K and 10 sccm of $N_2$ flow rate.

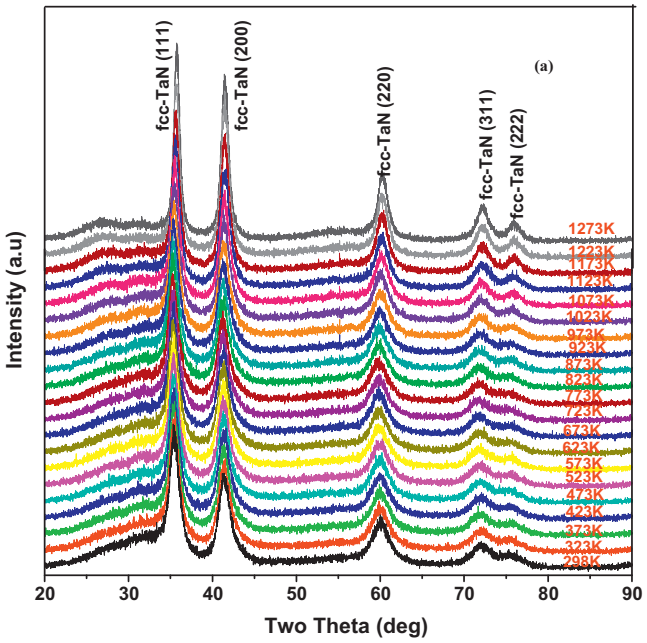


**Fig. 10.** HTXRD patterns of TaN films deposited at 773 K and 10 sccm.

with increasing temperature, e.g. the peak at $2\theta$ of 35.41° shifts to 35.29° at 723 K. The change of lattice constants of the cubic TaN with temperature is shown in Fig. 11. The broadness of the peaks indicates the nanocrystalline nature of the cubic crystals. Furthermore the $2\theta$ angle for each diffraction line of cubic TaN phase changes with increasing temperature due to the thermal expansion without phase transitions. This result is in agreement with the reported studies which states that $Ta_{1-x}N_x$ films, unlike $WN_x$, do not lose their N when subjected to high temperatures [28,29]. Fig. 12 shows the Rietveld analysis for the higher temperature (1073 K) XRD data of the TaN thin film. This analysis shows that there is no additional phase formation at these temperatures.

### 3.7. Thermal expansion study

For the purpose of calculating thermal expansivity, the corrected lattice parameter data with temperature ($K$) are fitted to a third-degree polynomial in the temperature increment ($T$-298).

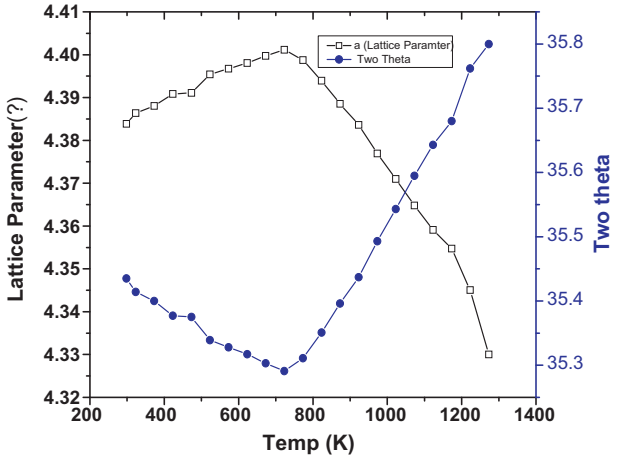


**Fig. 11.** Two theta peak shift of (2 0 0) plane at different temperatures.

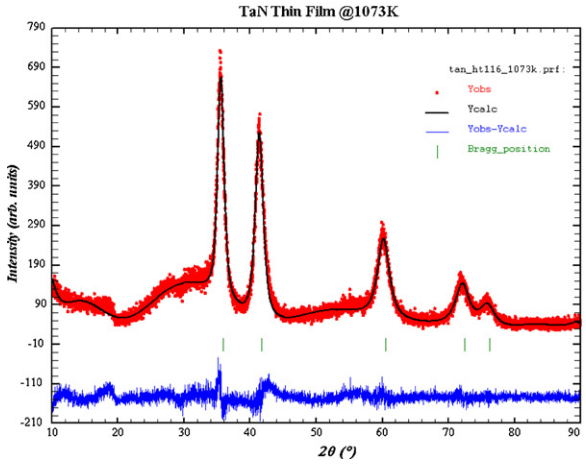


**Fig. 12.** The Rietveld analysis for TaN film at 773 K condition sample.

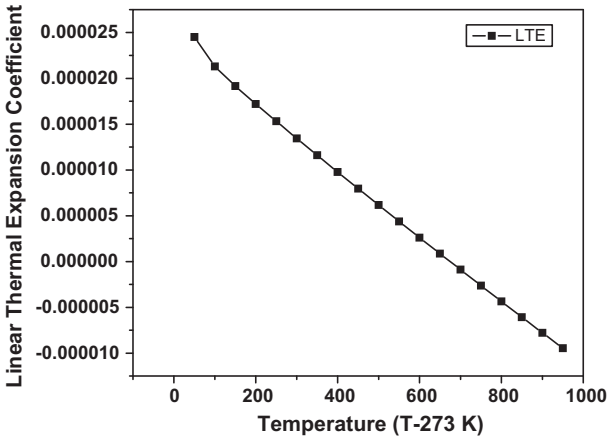


**Fig. 13.** Linear thermal coefficient of expansion vs. temperature.

The relevant fit expression (Eq. (2)) is given as

$$a = 4.37937 + 1.11319E - 4 \times (T\text{-}298) + (1.65354E - 7 \times (T\text{-}298)^2 + 9.14563E - 12) \times (T\text{-}298)^3 \quad (2)$$

The cell parameters of the cubic TaN, as deduced from the indexing of the XRD patterns are compiled in Table 1. Once the lattice parameter is known as a function of temperature, it is possible to estimate the mean (*á*L-mean) linear thermal expansion coefficients by using the equation (Eq. (3)),

$$\alpha m = \frac{1}{a_0\{(a_T - a_0)/(T - T_0)\}} \quad (3)$$

where $T_0$ is the room temperature (298 K) and $T$ is the temperature at which the measurements were done. The average thermal expansion coefficient value varies from $2.450 \times 10^{-5}$ to $-9.474 \times 10^{-6}$ in the ranges 298–1273 K respectively. The very strong negative thermal expansion (NTE) coefficient observed at temperatures above 1073 K is likely due to metal oxy nitride behaviors. The percentage of linear thermal expansion obtained for tantalum nitride computed is shown in Fig. 13. To the best of our knowledge, HT-XRD based lattice thermal expansion data for tantalum nitride is not available in the open literature. Cuong et al. reported that for TaN films annealed at nitrogen ambient, the TCR approached to near-zero value at higher annealing temperatures [29,30].

## 4. Conclusions

Structure, microstructure and morphology of the TaN thin films deposited on Si (1 0 0) substrates using pulsed dc reactive magnetron sputtering were studied as a function of nitrogen flow rate and substrate temperature. These studies lead to the following conclusions:

- The nitrogen flow rate has a significant influence on the phase, lattice parameter, surface morphology and crystallite size.
- The XRD analysis reveals that the films are polycrystalline in nature and are composed of single phasic fcc-TaN.
- The preferred crystalline orientation of the films changes from (1 1 1) to (2 0 0) direction at temperatures above 873 K.
- AFM images indicate a clear change in the surface morphology as a function of nitrogen addition. The films sputtered in pure argon atmosphere contain superposed round-shape grains, while the addition of nitrogen produces round particles.
- Thermal stability of the TaN film prepared at a substrate temperature of 773 K and with nitrogen flow rate of 10 sccm is found to be good up to 1123 K.

## Acknowledgments

The authors would like to thank R. Thirumurugesan and M. Jyothi for XRD Data collection. They also thank Dr. M. Vijayalakshmi, Head, Physical Metallurgy Division, Dr. T. Jayakumar, Director, Metallurgy and Materials Group and Dr. Baldev Raj, Director, IGCAR.

## References

[1] L.E. Toth (Ed.), Transition Metal Carbides and Nitrides, Academic Press, New York, London, 1971, p. 279.
[2] W. Lengauer, in: R. Riedel (Ed.), Nitrides and Carbonitrides: Handbook of Hard Materials, vol. 1, Wiley-VCH, Weinheim, 2000, pp. 202–252.
[3] J. Nazon, J. Sarradin, V. Flaud, J.C. Tedenac, N. Fréty, J. Alloys Compd. 464 (2008) 526–531.
[4] G.R. Lee, J.J. Lee, C.S. Shin, I. Petrov, J.E. Greene, Thin Solid Films 475 (2005) 45–48.
[5] C.A. Jong, J.Y. Gan, T.S. Chin, Jpn. J. Appl. Phys. 41 (2002) 5367–5371.
[6] C. Angelkort, A. Berendes, H. Lewalter, W. Bock, B.O. Kolbesen, Thin Solid Films 437 (2003) 108–115.
[7] D. Choi, P.N. Kumta, J. Am. Ceram. Soc. 90 (2007) 3113–3120.
[8] J. Nazon, J. Sarradin, V. Flaud, J.C. Tedenac, N. Frety, J. Alloys Compd. 464 (2008) p.526–531.
[9] L.B. Jonsson, T. Nyberg, I. Katardjiev, S. Berg, Thin Solid Films 365 (2000) 43–48.
[10] H.C. Barshilia, K.S. Rajam, Surf. Coat. Technol. 201 (2006) 1827–1835.
[11] N. Terao, Jpn. J. Appl. Phys. 10 (1971) 248–259.
[12] C.S. Shin, Y.W. Kim, D. Gall, J.E. Greene, I. Petrov, Thin Solid Films. 402 (2002) 172–182.
[13] M. Stavrev, D. Fischer, C. Wenzel, K. Drescher, N. Mattern, Thin Solid Films 307 (1997) 79–88.
[14] S. Tsukimoto, M. Moriyama, M. Murakami, Thin Solid Films 460 (2004) 222–226.
[15] W.H. Lee, J.C. Lin, C. Lee, Mater. Chem. Phys. 68 (2001) 266–271.
[16] F. Cheng, C. Jiang, J. Wu, Mater. Lett. 59 (2005) p.1530–1532.
[17] T. Elangovan, P. Kuppusami, R. Thirumurugesan, C. Sudha, E. Mohandas, D. Mangalaraj D., Mater. Sci. Eng. B 167 (2010) 17–25.
[18] Y.S. Jung, Appl. Surf. Sci. 22 (2004) 281–287.
[19] R.J. Hong, K. Helming, X. Jiang, B. Szyszka, Appl. Surf. Sci. 226 (2004) 378–386.
[20] G. Knuyt, C. Quaeyhaegens, J.D. Haen, L.M. Stals, Thin Solid Films 258 (1995) p.159–169.
[21] C.H. Ma, J.H. Huang, H. Chen, Thin Solid Films 446 (2004) 184–193.
[22] V.I. Parvulescu, C. Visinescu, V. Parvulescu, V. Marcu, F. Levy, Catal. Today 118 (2006) 433–439.
[23] J.W. Lee, S.K. Tien, Y.C. Kuo, Thin Solid Films 494 (2006) p.161–167.
[24] D.M. Zhang, L. Guan, Z.H. Li, G.J. Pan, H.Z. Sun, X.Y. Tan, L. Li, Surf. Coat. Technol. 200 (2006) 4027–4031.

[25] T. Elangovan, P. Kuppusami, R.P. George, C. Sudha, E. Mohandas, D. Mangalaraj, 1st Nano Today Conference, August 2–5, Singapore (Poster Presentation), 2009.
[26] E. Niu, L. Li, G. Lv, W. Feng, H. Chen, S. Fan, S. Yang, X. Yanga, Appl. Surf. Scil 253 (2007) pp.5223–5227.
[27] Q.Y. Zhang, X.X. Mei, D.Z. Yang, F.X. Chen, T.C. Ma, Y.M. Wang, F.N. Teng, Nucl. Instrum. Methods Phys. Res. B 127 (1997) 664–668.
[28] P. Lamour, P. Fioux, A. Arnaud Ponche, M. Michel Nardin, M.-F. Marie-France Vallat, P. Pierre Dugay, J.P. Brun, N. Moreaud, J.M. Pinvidi, Surf. Interface Anal. 40 (2008) 1430–1437.
[29] http://www.lib.ncsu.edu/theses/available/etd-07042002-121103/.
[30] N.D. Cuong, D.J. Kim, B.D. Kang, C.S. Kim, S.G. Yoon, J. Vac. Sci. Technol. B 24 (2006) 1398–1401.